TPGS/Phospholipids Mixed Micelles for Delivery of Icariside II to Multidrug-Resistant Breast Cancer

Jie Song, MSc[1,2], Houcai Huang, MSc[2], Zhi Xia, BSc[2], Yingjie Wei, PhD[2], Nan Yao, MSc[2], Li Zhang, MSc[2], Hongmei Yan, PhD[2], Xiaobin Jia, PhD[2], and Zhenhai Zhang, PhD[2]

Abstract

The biggest challenge for the treatment of multidrug resistant cancer is to deliver a high concentration of anticancer drugs to cancer cells. Icariside II is a flavonoid from *Epimedium koreanum* Nakai with remarkable anticancer properties, but poor solubility and significant efflux from cancer cells limited its clinical use. In our previous study, a self-assembled mixture of micelles (TPGS–Icariside II–phospholipid complex) was successfully constructed, which could substantially increase the solubility of Icariside II and inhibit the efflux on Caco-2 cells. In this study, we evaluate the anticancer effect of the mixed micelles encapsulating Icariside II (Icar-MC) on MCF-7/ADR, a multidrug-resistant breast cancer cell line. The cellular uptake of the micelles was confirmed by fluorescent coumarin-6-loaded micelles. The IC_{50} of Icar-MC in MCF-7/ADR was 2-fold less than the free drug. The in vitro study showed Icar-MC induced more apoptosis and lactate dehydrogenase release. Intravenous injection of Icar-MC into nude mice bearing MCF-7/ADR xenograft resulted in a better antitumor efficacy compared with the administration of free drug, without causing significant body weight changes in mice. The antitumor effect was further verified by magnetic resonance imaging and immunohistochemical assays for Ki-67, a proliferative indicator. Moreover, Icar-MC treatment also elevated Bax/Bcl-2 ratio and the expressions of cleaved caspase-3, -8, -9 and AIFM1 in tumors. This study suggests that phospholipid/TPGS mixed micelles might be a suitable drug delivery system for Icariside II to treat multidrug resistant breast cancer.

Keywords

micelles, multidrug resistance, Icariside II, MCF-7/ADR, P-glycoprotein

Introduction

The flavonoid compound Icariside II (also known as Baohuoside I), which is derived from the stems and leaves of *Epimedium koreanum* Nakai (Berberidaceae), has exhibited potential anticancer activities.[1,2] However, Icariside II possesses a poor solubility in both water and organic solvents. Furthermore, the significant efflux from cancer cells also limits its clinical application.

Self-assembled micelle system is recognized as one of the most promising strategies to deliver poorly soluble anticancer drugs.[3-5] In our previous study, a self-assembled mixture of micelles (TPGS–Icariside II–phospholipid complex) was constructed using phospholipid complex and TPGS (D-α-tocopheryl polyetheyene glycol 1000 succinate), which was capable of inhibiting the efflux and improving the solubility of Icariside II.[6] As an important component of the cell membrane, phospholipids can sustain membrane fluidity. They represent a well-known class of biocompatible and noncytotoxic biomolecules. Phospholipid complexes have been successfully applied to improve the permeability and bioavailability of drugs, such as clarithromycin and curcumin.[7,8] TPGS, containing a lipophilic nonpolar head and a hydrophilic tail, would be an ideal solubilizer to provide high drug encapsulation and emulsification efficiency for lipid-based drug delivery formulations.[9] Moreover, TPGS could reverse multidrug resistance (MDR) by inhibiting the P-glycoprotein (P-gp) pump.[10,11]

[1]School of Pharmacy, Nanjing University of Chinese Medicine, Nanjing, China
[2]Jiangsu Provincial Academy of Chinese Medicine, Shizi Street, Jiangsu, Nanjing, China.

Corresponding Author:
Xiaobin Jia and Zhenhai Zhang, Key Laboratory of Delivery Systems of Chinese Meteria Medica, Jiangsu Provincial Academy of Chinese Medicine, Shizi Street 100, Jiangsu, Nanjing 210028, China.
Email: jiaxiaobin2005@126.com; davidpharm@yahoo.cn

All these characteristics make them qualified surfactants to overcome drug efflux.[12] Breast cancer continues to be the most common malignancy diagnosed in women worldwide.[13] MDR is considered as one of the main reasons for the failure of cancer chemotherapy.[14] The principal mechanism of MDR is drug efflux from cancer cells by overexpressing P-gp.[15]

We assumed that phospholipid-TPGS micelles might be a promising platform for improving the therapeutic efficacy of Icariside II in drug-resistant cells. In this work, the in vitro and in vivo antitumor efficacy of Icar-MC against MDR breast cancer cells was estimated.

Materials and Methods

Cell Culture and Reagents

The human breast carcinoma cell lines MCF-7 and MCF-7/ADR (an ADR-resistant breast cancer cell line) were purchased from American Type Culture Collection and maintained in RPMI 1640 containing 10% fetal bovine serum, 2 mM L-glutamine, 1% penicillin-streptomycin (50 IU/mL and 50 μg/mL, respectively) at 37°C in an atmosphere of 5% CO_2. Icariside II was dissolved in dimethyl sulfoxide (DMSO) for in vitro experiments and was suspended in phosphate-buffered saline (PBS) with 0.2% sodium carboxymethylcellulose (CMC-Na) for in vivo experiments. Coumarin-6, Icariside II and 4′,6-diamidino-2-phenylindole (DAPI) was purchased from Sigma (St. Louis, MO). Icariside II-phospholipid complex was prepared by an anhydrous cosolvent reduction vaporization method as previously described.[6] All other chemicals were of high-performance liquid chromatography or reagent grade and used without further purification.

Uptake of Calcein-AM in MCF-7/ADR Cells

P-gp activity in the MCF-7 or MCF-7/ADR cells was firstly examined with the Multidrug Resistance Assay Kit (Molecular Probes, Eugene, OR), which evaluates the mean fluorescence of calcein AM accumulated in cells.[16] Cells were preincubated with increasing concentrations of cyclosporin A (10^{-5} to 0.1 mg/mL) for 30 minutes. P-gp substrates (Calcein-AM, 0.3 μM) were added and cells were further incubated for 30 minutes. At the end of incubation, intracellular fluorescence of P-gp substrates was quantified by a microplate reader (Bio-Rad iMark, Richmond, CA) at 488 nm. We further examined the P-gp activity in TPGS- or empty micelles-treated MCF-7/ADR cells. Calcein AM (0.3 μM) was added to the culture medium after cells had been incubated with TPGS (0.18 mg/mL) or empty micelles (0.2 mg/mL) for 15 minutes. Coincubation lasted for another 15 minutes. The fluorescence was measured using a microplate reader.

Cellular Uptake of the Coumarin-6-Loaded Micelles

Fluorescent coumarin-6-loaded micelle has been a successful model to investigate the cellular uptake of micelles.[17-19] Coumarin-6-loaded micelles were prepared by replacing Icariside II with coumarin-6 in the process of constructing Icar-MC. After treatment with coumarin-6-loaded micelles (6 μM) for 30 minutes, the cells were washed with PBS and then the nuclei were counterstained by DAPI for 10 min. The cells were washed again for fluorescence imaging.

In Vitro Cytotoxicity Study

In vitro cytotoxicity was determined using MTT assay. MCF-7/ADR cells (2×10^4/well) were treated with free Icariside II, Icar-MC (0-40 μM) or empty micelles (0.2 mg/mL) for 12, 24, 48 hours, respectively. The absorbance at 570 nm was used to assess the relative cell viability from 3 independent experiments.

Lactate Dehydrogenase Release

The MCF-7/ADR cells (1×10^6 cells/mL) were treated with Icar-MC or Icariside II at a concentration range of 0 to 40 μM for 12 hours. Released lactate dehydrogenase (LDH) in the media was measured with a cytotoxicity kit (Promega, Madison, WI) with absorbance at 340 nm.

Analysis of Cell Apoptosis

After incubation with Icar-MC or Icariside II (25 μM) for 24 hours, the cells (1×10^6 cells/mL) were trypsinized, washed with cold binding buffer, and suspended in Annexin V-Alexa Fluor 488 binding buffer (200 μL) for 15 minutes in darkness. The cells were diluted with binding buffer at a total volume of 400 μL and analyzed immediately by flow cytometry. Cells in the lower right quadrant represented apoptosis and in the upper right quadrant represented necrosis or postapoptotic necrosis.

Efficacy Study in Xenografts in Mice

Athymic nude mice (18-20 g) were obtained from the SLAC Lab Animal Center of Shanghai (Shanghai, China). They were maintained on a 12-hour light/dark cycle at the temperature of 25°C ± 2°C and relative humidity of 50% ± 10% with water ad libitum. This study and the experimental protocols were approved by the Institutional Animal Care and Use Committee (IACUC) of Jiangsu Provincial Academy of Chinese Medicine under the approval number JPA-081210-8.

MCF-7/ADR cells were injected subcutaneously into the flank area of female nude mice. On day 0 (5 days after cell implantation), tumor sizes reached an average of 75 mm³,

and mice were randomly divided into 4 groups (n = 8): group 1 (saline); group 2 (free Icariside II at 10 mg/kg, in PBS with 0.2% CMC-Na); group 3 (empty micelles at 100 mg/kg, in PBS, pH 7.4); and group 4 (Icar-MC, containing the same dose of Icariside II as group 2, in PBS, pH 7.4). Treatments via intravenous injections or oral gavage began on day 1. Mice in groups 1 and 2 were dosed through oral gavage every 3 days for a total of 8 times (finished on day 24). Mice in groups 3 and 4 were injected intravenously every 3 days for a total of 8 injections (finished on day 24). Tumors were measured thrice a week with an electronic caliper by using the formula: Tumor volume (mm^3) = length $\times$ width^2/2. The experiment was ended at day 34, 10 days after the last treatment (day 24), and all the mice left were euthanized. During the experiment, mice with tumor size exceeding 1000 mm^3 were also euthanized. Tumors were isolated immediately for further Western blotting and immunohistochemical assays after euthanasia.

Magnetic Resonance Imaging

The nude mice were subjected to magnetic resonance imaging (MRI) (Excite Echospeed HD 1.5T, GE MRI system, Waukesha, WI) on day 34.[20] Coronal position, transverse section (T1WI, T2WI) and diffusion-weighted imaging (DWI) were employed using a matrix of 224 × 192 pixels, and a slice thickness of 3 mm, interval 0.2 mm, field of view 10 cm × 10 cm, 2NEX. T1WI: SE array, TR (repetition time)/TE (echo time) = 550 ms/24ms. T2WI: FSE array, TR/TE = 2920 ms/88 ms. DWI: SE/EPI, TR/TE = 4000 ms/71.6 ms, matrix = 64 × 96, 8NEX.

Western Blot Analysis

The protein levels in tissue homogenates were assessed with the use of methods described previously.[21] After the indicated treatment, tissue homogenates were lysed in extract buffer. Equal amounts of proteins from each set of experiments were separated by sodium dodecyl sulfate–polyacrylamide gel electrophoresis. The gel was transferred to membrane and probed with either P-gp, Bax, caspase-3, -8, -9, PARP, FADD, AIFM1, Bcl-2 antibodies, each obtained from Cell Signaling Technologies (Beverly, MA). The protein bands were visualized by enhanced chemiluminescence detection kit (Beyotime, Shanghai, China). Densitometric measurements of the scanned bands were performed using Image pro plus (IPP) software program. Data were normalized to β-actin.

Immunohistochemical Studies

Sections (5 μm) from paraformaldehyde-fixed tissues were dewaxed with xylene and ethanol and then washed in distilled water. After incubating in hydrogen peroxide to quench endogenous peroxidase activity, the slides were heated at 100°C to retrieve antigens. The slides were incubated with anti-Ki-67 antibody from Nanjing Bioworld Biotech Co Ltd. (Nanjing, China) for 1 hour, followed by incubation with horseradish peroxidase–conjugated secondary antibody. Sections were then incubated with developing solution, and counterstained with hematoxylin. Color was fixed with acid alcohol and dehydration steps. Immunoreactivity was identified as brown nuclear or cytoplasmic labeling in tumors counterstained with hematoxylin.

Statistical Methods

The experiments exposed were representative from three independent experiments. All descriptive statistics, including mean ± SD, were performed. Student's *t* test was used to evaluate differences between the control group and each treatment group in all in vitro studies. For multigroup comparisons, a 2-way analysis of variance test was used. To compare animal survivals, the log-rank test was used and the results were shown with Kaplan-Meier curves.

Results

P-glycoprotein Activities in MCF-7/ADR Cells

Calcein AM was used as a substrate to evaluate the activity of P-gp in the presence of increasing concentration of cyclosporin A (a competitive inhibitor of P-gp). Previous research reported that cyclosporin A displayed dose-dependent inhibition of P-gp-mediated calcein AM efflux.[22] Therefore, greater retention of calcein AM means greater inhibitory effects on the P-gp activity. As shown in Figure 1A, high concentration of cyclosporin A induced retention of calcein in MCF-7/ADR cells but not in MCF-7 cells, signifying that P-gp was much more active in MCF-7/ADR cells. Moreover, high level of P-gp proteins was detected in MCF-7/ADR cells, as shown in Western blot assays (Figure 1B).

We further examined the P-gp activity in TPGS- or empty micelles-treated MCF-7/ADR cells. Characterization of Icar-MC has been carried out in our previous research, demonstrating that this formulation was able to increase the solubility and the permeability of Icariside II. New experimental data from batches in this study are shown in Table 1. The weight ratio of TPGS:empty micelle was 9:10 when constructing Icariside II-loaded mixed micelles. The relative fluorescence value for retention of calcein AM was 69.5 ± 1.8 at the control group, 122.3 ± 12.8 in TPGS group (0.18 mg/mL), and 113.4 ± 11.5 in empty micelles group (0.2 mg/mL). It is obvious that TPGS or empty micelles would increase calcein AM retention in MCF-7/ADR cells (Figure 1C). However, both treatments failed to affect P-gp protein levels in MCF-7/ADR cells (Figure 1D).
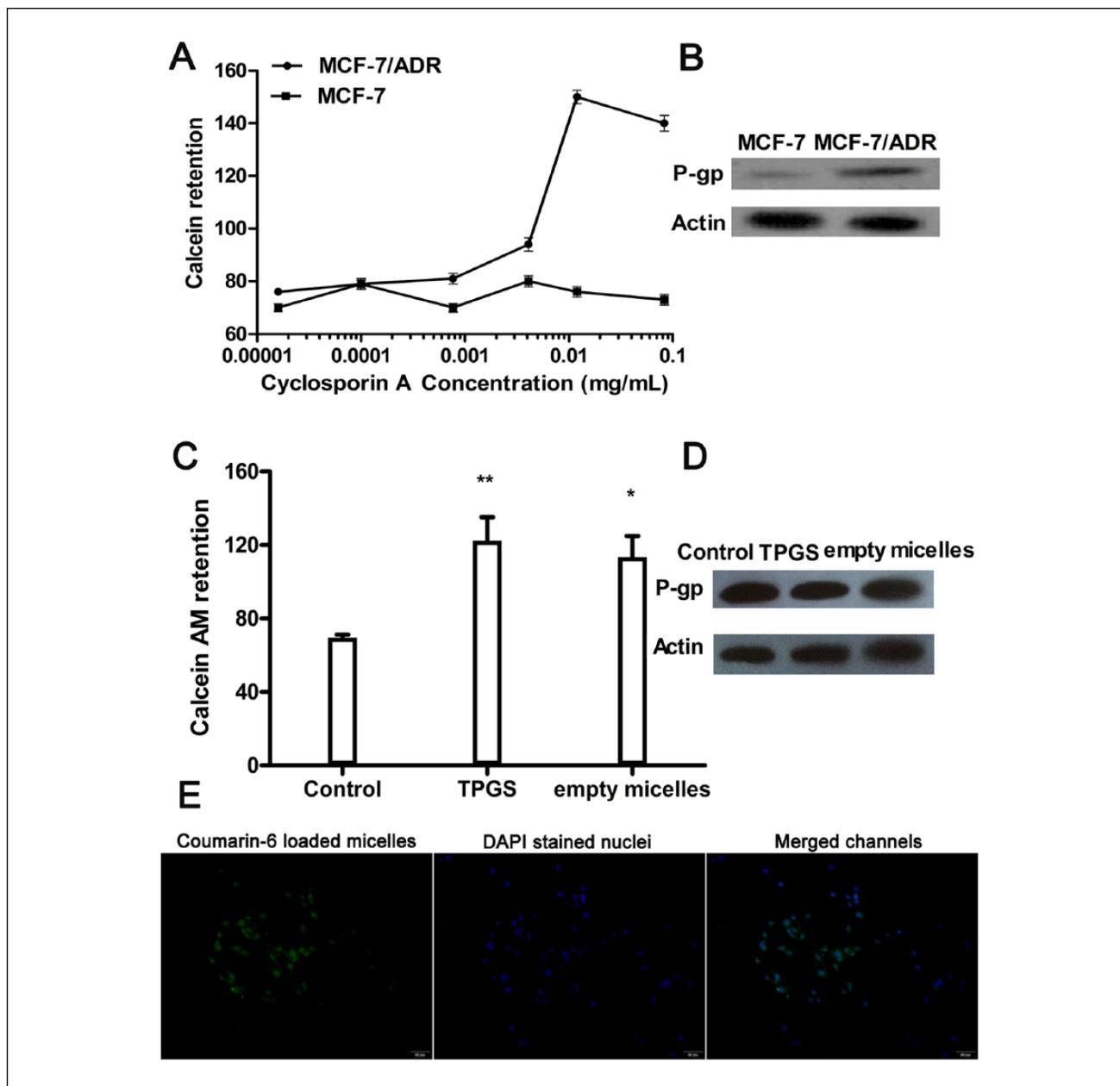
Figure 1. Activity of P-glycoprotein (P-gp) and cellular uptake of micelles. (A) P-gp activity was determined by retention of calcein AM in the multidrug resistance assay. (B) P-gp protein expression was determined by Western blotting. (C) P-gp activity after treatment with TPGS (0.18 mg/mL) or empty micelles (0.2 mg/mL) by detecting cellular accumulation of calcein AM in MCF-7/ADR cells. Greater numbers suggest greater inhibitory effects on the P-gp activity (*$P < .05$, **$P < .01$ vs control). (D) P-gp protein expression was determined by Western blotting. (E) Determination of cellular uptake of micelles by fluorescence microscope on MCF-7/ADR cells. The green fluorescence from coumarin-6-loaded micelles distributed in cytoplasm; the blue fluorescence from DAPI-stained nuclei.

In Vitro Cellular Uptake

After incubation with the coumarin-6-loaded TPGS micelles for 30 minutes, images of MCF-7/ADR cells are shown in Figure 1E. The green fluorescence is emitted by coumarin-6 and the blue fluorescence is obtained from the DAPI channel. From the images, DAPI-stained nuclei are circumvented by green fluorescence. This proves that micelles have entered into the cellular cytoplasm.

In Vitro Cytotoxicity

The in vitro cytotoxicity of free Icariside II and Icariside II-loaded mixed micelles in MCF-7/ADR cells was examined

Table 1. Physicochemical Characteristics of Icariside II–Loaded Mixed Micelles (Mean ± SD, n = 3 Different Batches).

	Size (nm)	Zeta Potential (mV)	Entrapmet Efficiency (%)	Solubility (µg/mL)
Icar-MC	95.22 ± 6.7	−17.3 ± 3.2	86.5 ± 4.0	347.5
Icariside II	—	—	—	12.8

with MTT assay. The result indicates that Icar-MC has advantages in achieving higher cytotoxicity than the free drug. The IC_{50} of Icar-MC (12.6 ± 0.6 µM) in MCF-7/ADR cells was found to be 2-fold less than the free Icariside II (25.2 ± 0.7 µM) ($P < .01$) after 24-hour incubation. The IC_{50} of Icar-MC (8.7 ± 0.4 µM) was 1.5-fold less than the free drug (13.3 ± 0.5 µM) ($P < .05$) after 48-hour incubation (Figure 2A). The cytotoxicity of empty micelles was evaluated on MCF-7/ADR to discriminate the effect of Icar-MC from empty micelles. Our results confirmed that the empty micelles at 0.2 mg/mL are noncytotoxic to MCF-7/ADR cells. The P-gp inhibiting effect by the TPGS makes these micelles a better nanocarrier for Icariside II delivery. It allows sustaining the drug concentration inside the cell, resulting in a more potent cytotoxic effect. Icar-MC-treated cells had higher level of LDH release compared to free Icariside II at all concentrations (0-40 µM) (Figure 2B). Statistical analysis showed that the difference in LDH release between Icariside II and Icar-MC was significant at 20 and 40 µM. In accordance with MTT assay, Icar-MC treatment resulted in higher apoptotic cells than Icariside II (Figure 2C). This experiment was repeated three times, and the difference is statistically significant ($P < .05$).

Assessment of In Vivo Therapeutic Efficacy

The tumor volumes of MCF-7/ADR xenograft and weights of nude mice were measured thrice a week. The tumor volume kept increasing in the mice treated with saline (Figure 3, Table 2). On day 24 (the last treatment), 5 out of the 8 mice with tumors exceeding the size limit of 1000 mm³ were euthanized. The rest of the mice in the saline group were euthanized successively once the tumors reached the size limit. Empty micelles (200 mg/kg) exhibited no tumor inhibition on nude mice. On day 25, one death occurred in the empty micelles group due to tumor burden. None of the animals in this group survived to the end of the study (day 34, 10 days after they were given the last treatment).

Icariside II is almost insoluble in aqueous solutions; therefore, it was orally given in PBS with 0.2% CMC-Na at pH 7.4. Free Icariside II (10 mg/kg) exhibited weak inhibition on tumor growth, without statistical significance compared to the saline group. In the Icariside II group, three mice received euthanasia successively due to exceeding the tumor size limit. Five mice survived to the end of the study in the Icariside II group (day 34).

Strong suppression of tumor volume was observed in animals receiving Icar-MC (10 mg/kg of Icariside II basis),

compared to the saline group ($P < .05$). At the end of the study, the mean tumor size was 285 mm³ from an initial average volume of 75 mm³. Two out of the 8 mice had obvious tumor regression. There is a statistical significance between free Icariside II and Icariside II-loaded micelles ($P < .05$). MRI analysis of the mice harvested at the end of the experiment demonstrated that the tumor volumes differed significantly between the Icariside II and Icar-MC groups (Figure 3C).

To estimate the adverse effects of the mixed micelle formulations, body weight of the mice was also recorded during the treatment and the results are shown in Figure 3D. It can be easily observed that the average body weight of the mice in all groups showed similar trends: slow increase in the initial 7 days, quick increase between 8 and 12 days, and unchanged afterward.

Immunohistochemical Assays

We carried out immunohistochemistry assay in tumors to examine the cell proliferation indicator Ki-67. As expected, Ki-67-positive cells were decreased in Icar-MC-treated tumors, indicating the reduction of proliferated cells (Figure 4). These findings strengthened the conclusion that Icar-MC had greater therapeutic efficacy than Icariside II alone.

Expressions of Apoptosis-Related Proteins

We then investigated the molecular mechanisms responsible for the antitumor effect of Icar-MC. β-actin is not a good loading control when apoptosis is induced. We used Hsc70 as the loading control which was less sensitive to caspase cleavage. Icar-MC enhanced the levels of Bax, cleaved caspase-8, -9, -3, cleaved PARP, and AIFM1 compared with vehicle; decreased the expressions of Bcl-2 in tumor tissues (Figure 5). Icar-MC induced apoptosis involving both the intrinsic and extrinsic signaling pathways. Free Icariside II also displayed a tendency to modulate the expressions of apoptosis-related proteins, but to a lesser extent. Thus, mixed micelles made of TPGS and phospholipid complexes allowed for a strong pro-apoptotic effect of Icariside II.

Discussion

This study was designed to investigate whether self-assembled micelles can enhance Icariside II absorption and overcome MDR. We have shown several important
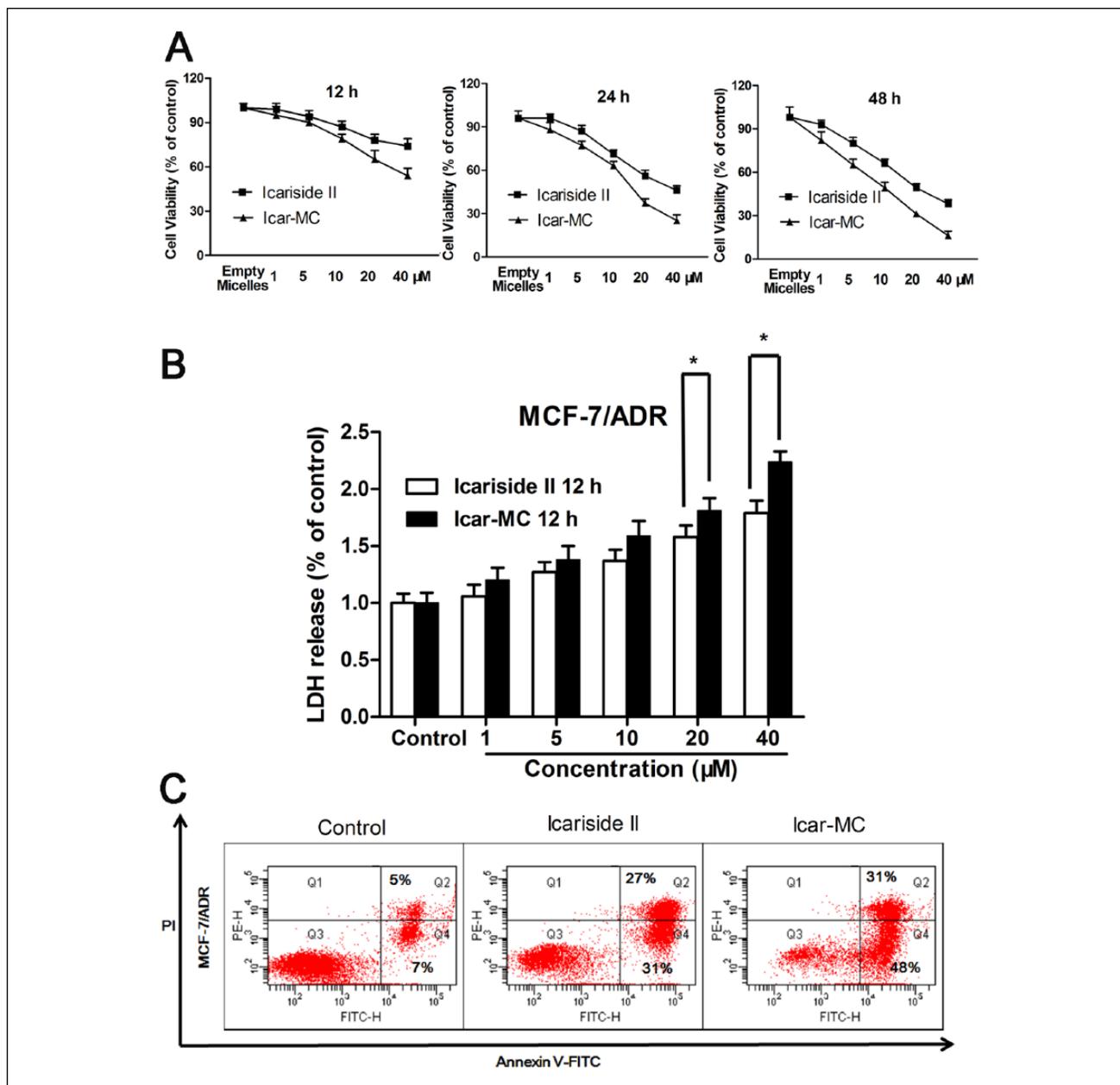
Figure 2. In vitro cytotoxicity assays. (A) MTT assay. Cells were incubated with Icariside II, Icar-MC (1-40 µM) or empty micelles (0.2 mg/mL) for 12, 24, and 48 hours to evaluate cytotoxicity by MTT assay. (B) Lactate dehydrogenase (LDH) release. The cells were treated with Icariside II and Icar-MC for 12 hours, before analyzing the media for LDH release (*$P < .05$, **$P < .01$ versus control). (C) Apoptosis. Cells were incubated with Icariside II and Icar-MC (25 µM) for 24 hours to evaluate apoptosis by flow cytometry.

points: (*a*) TPGS and empty micelles inhibited P-gp activity, and in vitro cellular uptake of fluorescent coumarin-6-loaded micelles was confirmed; (*b*) the micelle strategy was able to enhance the cytotoxicity of Icariside II on MCF-7/ADR cells, and inducing apoptosis is the major mechanism responsible for the cytotoxicity; (*c*) a remarkable effect on tumor inhibition was observed in MCF-7/ADR xenografts by Icar-MC; and (*d*) Icar-MC regulated the expressions of apoptosis-related proteins in vivo.

Most MDR cases are largely attributed to the overexpression of P-gp, a 170-kDa plasma membrane ATPase. P-gp is expressed in approximately 40% of breast cancer tumors; and such tumors are 3 times less likely to respond to chemotherapy than those that do not express P-gp.[23] As a broad-spectrum multidrug efflux pump, P-gp can recognize a variety of structurally unrelated chemotherapeutic agents, called P-gp substrates.[24] Our study showed that MCF-7/ADR cells expressed higher levels of P-gp and more
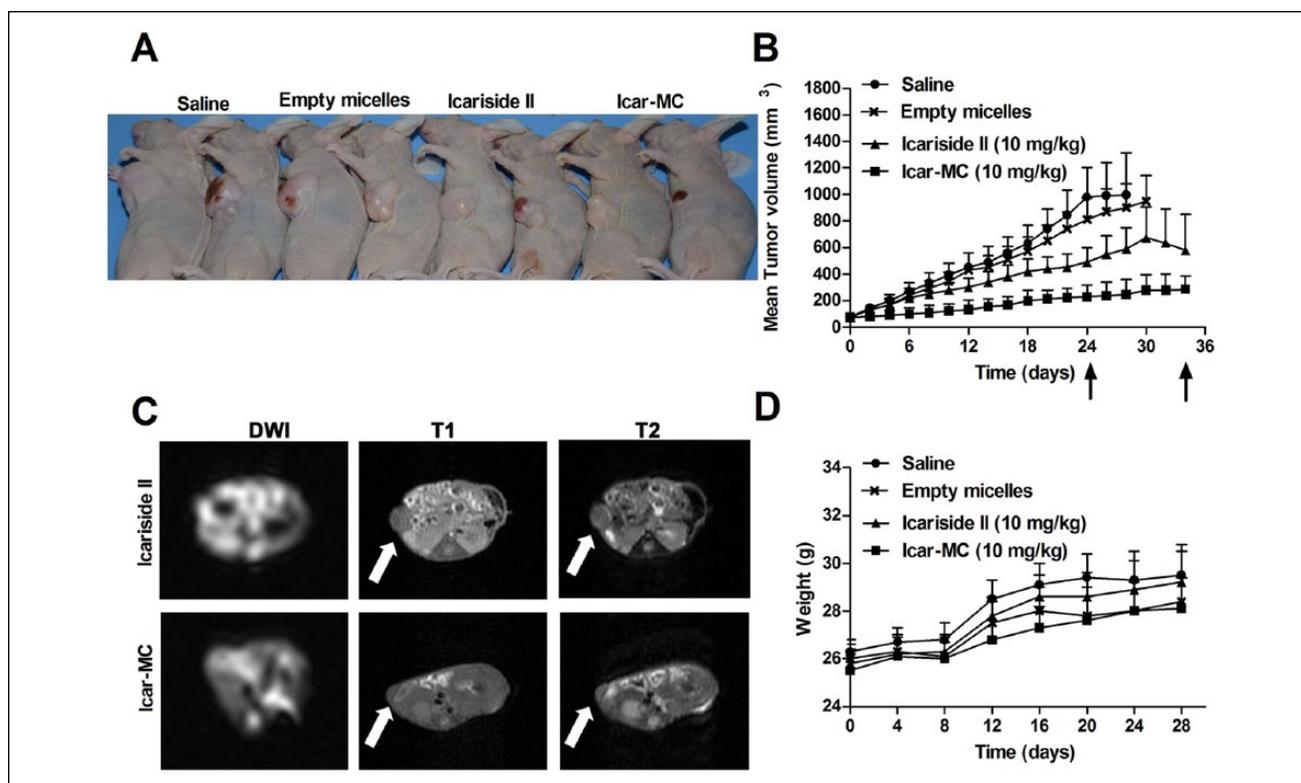
Figure 3. In vivo therapeutic efficacy of Icar-MC in mice bearing MCF-7/ADR xenograft. (A) Mice with representative tumor xenografts are shown. (B) Mean tumor volumes as functions of time. Arrows indicate the last treatment at day 24 and the end of the experiment at day 34. Empty micelles were injected intravenously at 100 mg/kg. (C) Examples of the transverse sections of high-resolution magnetic resonance images of the tumor xenografts were shown here for illustration. Arrows, tumor location. (D) Body weight changes for the tumor-bearing mice after various formulations were given to mice on the indicated days.

Table 2. Antitumor Efficacy Studies in Nude Mice Bearing MCF-7/ADR Xenograft.

	N_{end} [a]	N_{deas}/N_{eu} [b]	Tumor Volume (mm³)		N_{zero} [c]	P [d]	P [e]
			Mean	Median			
Icariside II (10 mg/kg)	5	0/3	580	610	0	.21	—
Empty micelles	0	1/7	950	947	0	.33	.25
Icar-MC (10 mg/kg)	8	0/0	285	327	2	.03	.04
Saline	0	0/8	995	1123	0	—	.32

[a]N_{end} is the number of animals surviving at the end of the study.
[b]N_{dea} is the number of treatment-related deaths and N_{eu} is the number of animals euthanized with the tumor size more than 1000 mm³.
[c]N_{zero} is the number of animals with tumor size close to zero at the end of the study (n = 8 mice/group).
[d]*P* means *P* versus saline.
[e]*P* means *P* versus Icariside II.

activity of P-gp than MCF-7 cells, which is in accordance with previous research that the P-gp efflux pump is essential in the multidrug-resistant phenotype of the MCF-7 cells.[25]

The use of TPGS, as a drug delivery vehicle to treat MDR cancers is a rapidly developing area. TPGS can prevent P-gp-mediated efflux and elevate drug bioavailability. Furthermore, TPGS has been used as a sole excipient and a brilliant emulsifier to reverse paclitaxel drug resistance in ovarian cancer cells.[26,27] Also, TPGS itself has cancer-fighting properties, though the mechanism is unclear. In light of these findings, TPGS is incorporated into Icariside II–phospholipid complex to produce the mixture of micelles. In this study, the mixed micelles successfully reduced the efflux of Icariside II in Caco-2 cell monolayers.[6] TPGS upregulated calcein AM retention level in MCF-7/ADR
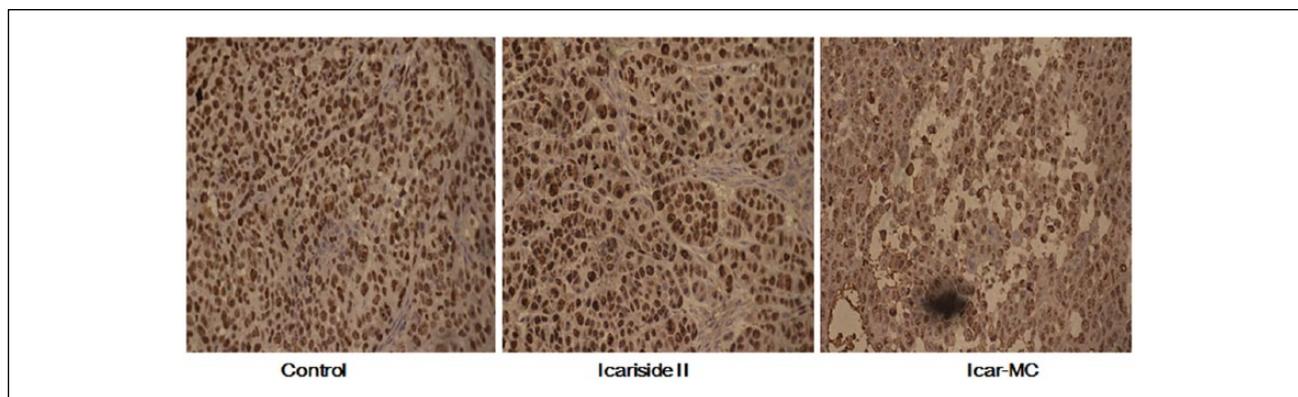
Figure 4. Antitumor effect of Icar-MC in nude mice. Icar-MC treatment inhibited tumor-cell proliferation as determined by immunohistochemistry for Ki-67. Bars show standard errors.
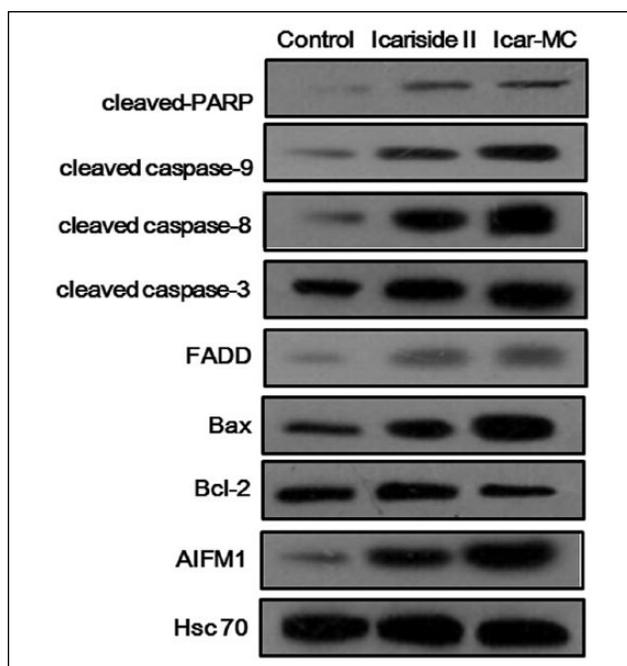
Figure 5. Effects on the apoptosis-related protein expressions. The nude mice bearing MCF-7/ADR xenografts were treated with the indicated doses of Icariside or Icar-MC for total 8 doses. The expression of proteins from tumor homogenates was analyzed by Western blotting.

cells without changing P-gp protein levels. Calcein AM was used as a substrate to evaluate P-gp activity. Greater retention of calcein AM means greater inhibitory effects on the P-gp activity. Here, it can be inferred that mixed micelles inhibited the P-gp activity directly rather than modulating P-gp protein expressions.

As expected, data obtained from in vitro MTT study showed that Icar-MC exhibited stronger inhibitory effect on the proliferation of MCF-7/ADR cells than Icariside II.

Also in this work, the progressive changes of the tumor volume in the MCF-7/ADR xenografted nude mice confirmed the higher antitumor activity of Icar-MC as compared to free drug at a comparable dosage of Icariside II. Namely, the behavior of Icar-MC in vivo correlated well with their in vitro interaction with tumor cells. As a tumor-fighting drug, the cellular uptake of Icariside II is a predominant process for its therapeutic efficacy. Previous research has emphasized that the addition of the TPGS into polymeric nanoparticles can increase the cellular uptake in tumor.[28] In vitro cellular uptake results obtained here also confirmed this. This formulation promoted intracellular accumulation of Icariside II in cells, which could explain the improvement of the anticancer efficiency in vitro and in vivo.

In the in vivo experiment, free drug is applied orally and the mixed micelle intravenously. Plasma concentrations of Icariside II from the 2 formulations were reported in our previous work. The average value of C_{max} is 298.87 ng/mL after oral administration of free drug, while the average value of C_{max} reached 798.65 ng/mL after oral administration of Icar-MC.[6] Here, we concluded that except for the more significant uptake of Icar-MC over Icariside II by cancer cells and overcoming drug resistance, the improved plasma concentration of Icariside II might also contribute to the difference in anticancer efficacies. Moreover, the in vivo activity of Icariside II-loaded micelles may also be improved by their augmented accumulation in tumor tissues due to the enhanced permeability and retention effect. The tissue concentration of free Icariside II and Icar-MC should be evaluated in our future study to elucidate the effect of enhanced tumor accumulation.

In conclusion, this study has identified a novel drug delivery system, self-assembled micelle for encapsulation and delivery of Icariside II in P-gp-mediated drug-resistant cancers. The study provides a rationale for the continued investigation of Icar-MC as a promising anticancer therapy.

Authors' Note

Declaration of Conflicting Interests

Funding

References

1. Song J, Shu L, Zhang Z, et al. Reactive oxygen species-mediated mitochondrial pathway is involved in Baohuoside I-induced apoptosis in human non-small cell lung cancer. *Chem Biol Interact*. 2012;199:9-17.

2. Lee KS, Lee HJ, Ahn KS, et al. Cyclooxygenase-2/prostaglandin E2 pathway mediates icariside II induced apoptosis in human PC-3 prostate cancer cells. *Cancer Lett*. 2009;280:93-100.

3. Kim JO, Kabanov AV, Bronich TK. Polymer micelles with cross-linked polyanion core for delivery of a cationic drug doxorubicin. *J Control Release*. 2009;138:197-204.

4. Liu J, Pang Y, Huang W, Zhu X, Zhou Y, Yan D. Self-assembly of phospholipid-analogous hyperbranched polymers nanomicelles for drug delivery. *Biomaterials*. 2010;31:1334-1341.

5. Mu L, Elbayoumi TA, Torchilin VP. Mixed micelles made of poly(ethylene glycol)-phosphatidylethanolamine conjugate and D-α-tocopheryl polyethylene glycol 1000 succinate as pharmaceutical nanocarriers for camptothecin. *Int J Pharm*. 2005;306:142-149.

6. Jin X, Zhang ZH, Sun E, Tan XB, Zhu FX, Jia XB. A novel drug-phospholipid complex loaded micelle for baohuoside I enhanced oral absorption: in vivo and in vivo evaluations. *Drug Dev Ind Pharm*. 2013;39:1421-1430.

7. Maiti K, Mukherjee K, Gantait A, Saha BP, Mukherjee PK. Curcumin-phospholipid complex: preparation, therapeutic evaluation and pharmacokinetic study in rats. *Int J Pharm*. 2007;330:155-163.

8. Wu Z, Guo D, Deng L, Zhang Y, Yang Q, Chen J. Preparation and evaluation of a self-emulsifying drug delivery system of etoposide-phospholipid complex. *Drug Dev Ind Pharm*. 2011;37:103-112.

9. Mu L, Feng SS. PLGA/TPGS nanoparticles for controlled release of paclitaxel: effects of the emulsifier and drug loading ratio. *Pharm Res*. 2003;20:1864-1872.

10. Saxena V, Hussain MD. Polymeric mixed micelles for delivery of curcumin to multidrug resistant ovarian cancer. *J Biomed Nanotechnol*. 2013;9:1146-1154.

11. Simon S, Schubert R. Inhibitory effect of phospholipids on P-glycoprotein: cellular studies in Caco-2, MDCKII mdr1 and MDCKII wildtype cells and P-gp ATPase activity measurements. *Biochim Biophys Acta*. 2012;1821:1211-1223.

12. Collnot EM, Baldes C, Wempe MF, et al. Influence of vitamin E TPGS poly(ethylene glycol) chain length on apical efflux transporters in Caco-2 cell monolayers. *J Control Release*. 2006;111:35-40.

13. Siegel R, Naishadham D, Jemal A. Cancer statistics, 2012. *CA Cancer J Clin*. 2012;62:10-29.

14. Lukianova-Hleb EY, Belyanin A, Kashinath S, Wu X, Lapotko DO. Plasmonic nanobubble-enhanced endosomal escape processes for selective and guided intracellular delivery of chemotherapy to drug-resistant cancer cells. *Biomaterials*. 2012;33:1821-1826.

15. Chen LM, Liang YJ, Zhang X, et al. Reversal of P-gp-mediated multidrug resistance by bromotetrandrine in vivo is associated with enhanced accumulation of chemotherapeutical drug in tumor tissue. *Anticancer Res*. 2009;29:4597-4604.

16. Shieh MJ, Hsu CY, Huang LY, Chen HY, Huang FH, Lai PS. Reversal of doxorubicin-resistance by multifunctional nanoparticles in MCF-7/ADR cells. *J Control Release*. 2011;152:418-425.

17. Kutty RV, Feng SS. Cetuximab conjugated vitamin E TPGS micelles for targeted delivery of docetaxel for treatment of triple negative breast cancers. *Biomaterials*. 2013;34:10160-10171.

18. Pan J, Feng SS. Targeted delivery of paclitaxel using folate-decorated poly(lactide)-vitamin E TPGS nanoparticles. *Biomaterials*. 2008;29:2663-2672.

19. Ren H, Gao C, Zhou L, Liu M, Xie C, Lu W. EGFR-targeted poly(ethylene glycol)-distearoylphosphatidylethanolamine micelle loaded with paclitaxel for laryngeal cancer: preparation, characterization and in vitro evaluation [published online March 27, 2014]. *Drug Deliv*. doi:10.3109/10717544.2014.896057.

20. Nemeth JA, Harb JF, Barroso U Jr, He Z, Grignon DJ, Cher ML. Severe combined immunodeficient-hu model of human prostate cancer metastasis to human bone. *Cancer Res*. 1999;59:1987-1993.

21. Wei LH, Huang XR, Zhang Y, et al. Deficiency of Smad7 enhances cardiac remodeling induced by angiotensin II infusion in a mouse model of hypertension. *PLoS One*. 2013;8:e70195.

22. Ansbro MR, Shukla S, Ambudkar SV, Yuspa SH, Li L. Screening compounds with a novel high-throughput ABCB1-mediated efflux assay identifies drugs with known therapeutic targets at risk for multidrug resistance interference. *PLoS One*. 2013;8:e60334.

23. Trock BJ, Leonessa F, Clarke R. Multidrug resistance in breast cancer: a meta-analysis of MDR1/gp170 expression and its possible functional significance. *J Natl Cancer Inst*. 1997;89:917-931.

24. Kobori T, Harada S, Nakamoto K, Tokuyama S. Mechanisms of P-glycoprotein alteration during anticancer treatment: role in the pharmacokinetic and pharmacological effects of various substrate drugs. *J Pharmacol Sci*. 2014;125:242-254.

25. Li PY, Lai PS, Hung WC, Syu WJ. Poly(L-lactide)-vitamin E TPGS nanoparticles enhanced the cytotoxicity

of doxorubicin in drug-resistant MCF-7 breast cancer cells. *Biomacromolecules*. 2010;11:2576-2582.

26. Collnot EM, Baldes C, Schaefer UF, Edgar KJ, Wempe MF, Lehr CM. Vitamin E TPGS P-glycoprotein inhibition mechanism: influence on conformational flexibility, intracellular ATP levels, and role of time and site of access. *Mol Pharm*. 2010;7:642-651.

27. Liu Y, Huang L, Liu F. Paclitaxel nanocrystals for overcoming multidrug resistance in cancer. *Mol Pharm*. 2010;7:863-869.

28. Wang G, Yu B, Wu Y, Huang B, Yuan Y, Liu CS. Controlled preparation and antitumor efficacy of vitamin E TPGS-functionalized PLGA nanoparticles for delivery of paclitaxel. *Int J Pharm*. 2013;446:24-33.